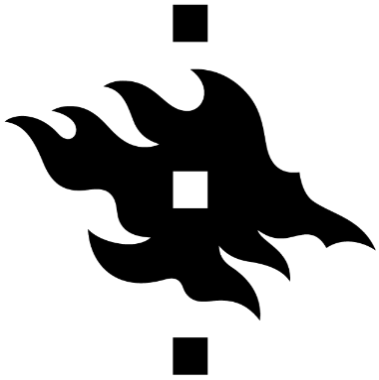

Monitoring Newborn and Infant Sleep Respiration and Heart Rate with a Wearable Sensor

Master's Thesis

Johanna Natalia Acosta Leinonen

Master's Programme in Neuroscience

Faculty of Biological and Environmental Sciences

University of Helsinki

April 2019

Supervisors: Sampsa Vanhatalo and Jukka Ranta

HELSINGIN YLIOPISTO
HELSINGFORS UNIVERSITET
UNIVERSITY OF HELSINKI

Tiedekunta – Fakultet – Faculty Biological and Environmental Sciences		Koulutusohjelma – Utbildingsprogram – Degree Programme Master's Programme in Neuroscience
Tekijä – Författare – Author Johanna Natalia Acosta Leinonen		
Työn nimi – Arbetets titel – Title Monitoring Newborn and Infant Sleep Respiration and Heart Rate with a Wearable Sensor		
Oppiaine/Opintosuunta – Läroämne/Studieinriktning – Subject/Study track Neuroscience		
Työn laji – Arbetets art – Level Master's Thesis	Aika – Datum – Month and year 04/2019	Sivumäärä – Sidoantal – Number of pages 39

Tiivistelmä – Referat – Abstract

Sleep is one of the most vital functions of newborns and infants, and it is essential for neuronal network development. Therefore, long-term sleep disturbances have been associated with growth delays and behavioral disorders. Commonly reported infant sleep disturbances, such as night awakenings and difficulties falling asleep, cause distress to parents. Yet, the development of infant sleep in the home environment has not been fully elucidated due to lack of objective measurement parameters. In the current study, we assessed the feasibility of a motion sensor, attached to wearable pants, and ECG textile electrodes to monitor sleep-related respiration and heart rate of newborns and infants. First, we compared signals recorded by the motion sensor's measurement channels to the standard respiratory piezo effort belt's signal during daytime EEG recordings. According to our results, the motion sensor's gyroscope proved to measure respiratory rate most accurately, while the ECG signal transmitted by the sensor was reliable in interpretable sections. We then provided wearable garments and smartphones to families with infants to assess overnight home-use. Our results indicate that different sleep states could likely be identified based on respiration fluctuation visible in the gyroscope's signals. Moreover, the wearable system was considered practical and easy to use by the parents. Future studies should focus on validating the sensor with clinically approved measures, in order to train the algorithms to automatically identify different sleep-wake states. By doing so, the wearable sensor could provide information on natural infant sleep structure development over long time periods. Additionally, clinical validation of the sensor may result in the development of a companion diagnostic tool for infant cardiorespiratory and movement disorders.

Avainsanat – Nyckelord – Keywords
Newborn, Infant, Sleep, Respiration, Electrocardiography, Polysomnography, Wearables, Motion sensor, Piezo sensor

Ohjaaja tai ohjaajat – Handledare – Supervisor or supervisors
Sampsa Vanhatalo and Jukka Ranta

Säilytyspaikka – Förvaringställe – Where deposited

Muita tietoja – Övriga uppgifter – Additional information

HELSINGIN YLIOPISTO
HELSINGFORS UNIVERSITET
UNIVERSITY OF HELSINKI

Tiedekunta – Fakultet – Faculty Bio- ja ympäristötieteellinen tiedekunta	Koulutusohjelma – Utbildingsprogram – Degree Programme Neurotieteen maisteriohjelma	
Tekijä – Författare – Author Johanna Natalia Acosta Leinonen		
Työn nimi – Arbetets titel – Title Vastasyntyneen ja imeväisikäisen vauvan unenaikaisen hengitys- ja syketaajuuden tarkkailu puettavalla liikeanturilla		
Oppiaine/Opintosuunta – Läroämne/Studieinriktning – Subject/Study track Neurotiede		
Työn laji – Arbetets art – Level Maisterintutkielma	Aika – Datum – Month and year 04/2019	Sivumäärä – Sidoantal – Number of pages 39

Tiivistelmä – Referat – Abstract

Vastasyntyneelle ja imeväisikäiselle nukkuminen on elintärkeä toiminto, ja se on välttämätöntä aivoverkkojen kehitykselle. Tiedetään, että huono unenlaatu aiheuttaa pitkällä tähtäimellä muun muassa kasvun hidastumista ja käyttäytymisongelmia. Imeväisikäisillä melko yleisesti esiintyvät unihäiriöt, kuten yöheräily ja nukahtamisvaikeudet aiheuttavat merkittävää rasitusta ja huolta vanhemmille. Objektiivisen mittausmenetelmän puutteen vuoksi ei ole kuitenkaan voitu selvittää imeväisikäisen unen kehittymistä kotiolosuhteissa. Tässä tutkimuksessa tarkasteltiin puettaviin pöksyihin kiinnitetyn liikeanturin ja EKG-kangaselektrodien soveltuvuutta vastasyntyneiden ja imeväisikäisten vauvojen unenaikaisen hengityksen ja sykkeen tarkkailuun. Tutkimuksen ensimmäisessä vaiheessa päiväaikaisten uni-EEG-tutkimuksien yhteydessä verrattiin liikeanturin mittauskanavien rekisteröimiä mittauskäyriä pietsoanturilla varustettuun hengitysvyöhön. Saatujen tutkimustuloksien perusteella liikeanturin gyroskooppi osoittautui tarkimmaksi hengitystaajuutta mittaavaksi parametriksi, kun taas anturin välittämä EKG-signaali oli tulkintakelpoisin osin luotettavaa. Tutkimuksen toisessa vaiheessa vauvaperheille annettiin unipöksyt ja älypuhelimet kotiin arvioidaksemme yön yli kestävää kotikäyttöä. Tutkimustulokset viittaavat siihen, että eri unitilojen tunnistaminen hengityksen vaihtelusta olisi todennäköisesti mahdollista gyroskooppisignaalista. Vanhemmilta saadun palautteen perusteella unipöksyjä pidettiin käytännöllisinä ja helppokäyttöisinä. Tulevissa tutkimuksissa tulisi keskittyä liikeanturin validointiin kliinisesti hyväksyttyjen mittausparametrien avulla, jotta algoritmeja voisi opettaa tunnistamaan eri uni-valve rytmejä automaattisesti. Näin puettava liikeanturi voisi tarjota tietoa vauvan luonnollisen unirakenteen kehittymisestä pitkällä aikavälillä. Lisäksi anturin kliininen validointi voisi mahdollistaa imeväisikäisten kardiorespiratoristen ongelmien ja liikehäiriöiden diagnostisen lisätyökalun kehittämisen.

Avainsanat – Nyckelord – Keywords
Vastasyntynyt, Imeväisikäinen, Uni, Hengitys, Elektrokardiografia, Polysomnografia, Puettavat, Liikeanturi, Pietsoanturi

Ohjaaja tai ohjaajat – Handledare – Supervisor or supervisors
Sampsa Vanhatalo ja Jukka Ranta

Säilytyspaikka – Förvaringställe – Where deposited

Muita tietoja – Övriga uppgifter – Additional information

Table of Contents

Abbreviations

ACC	Accelerometer
AS	Active sleep
BLE	Bluetooth Low Energy
ECG	Electrocardiography
EEG	Electroencephalography
EMG	Electromyography
EOG	Electrooculography
GYRO	Gyroscope
HF	High frequency
HR	Heart rate
HRV	Heart rate variability
MAGN	Magnetometer
ms	Milliseconds
MS	Movesense sensor
MEMS	Microelectromechanical system
NREM	Non rapid eye movement
PLV	Phase locking value
PSG	Polysomnography
QS	Quiet sleep
REM	Rapid eye movement
RESP	Respiratory piezo effort
RIP	Respiratory inductance plethysmography
RMSSD	Root mean square of successive differences
RR	Respiratory rate
RSA	Respiratory sinus arrhythmia
SNR	Signal-to-noise ratio

1. Introduction

Sleep is described as a reduction in consciousness and absence of response to external stimuli (Cirelli & Tononi 2008). Yet, it is an active neurophysiological process and the main activity of the developing brain (Bathory & Tomopoulos 2017). Fetuses and neonates spend most of their day asleep, which means that adequate sleep is specifically important for them (van den Hoogen et al., 2017). While the main purpose of sleep remains elusive (Bathory & Tomopoulos 2017), research has provided various hypotheses for the underlying causes of sleep. These include neuronal plasticity, learning and memory and adaptation to a circadian environment (Assefa et al., 2015; Skeldon et al., 2016). Moreover, sleep deprivation studies have highlighted the significance of sleep on the roles of the cardiovascular, immune (Faraut et al., 2012), musculoskeletal (Buxton et al., 2012) and metabolic (Dattilo et al., 2012) systems. Sufficient sleep is fundamental for normal growth and development in children, and it is also linked to predictors of health in adult life (Bathory & Tomopoulos 2017).

1.1 Infant Sleep Development and Phenomenology

The first five years of life represent a period of rapid and dynamic transformation in sleep duration, quality and architecture (Bathory & Tomopoulos 2017; Tham et al., 2017). At birth, newborns have immature circadian rhythms characterized by numerous short sleep intervals that are interfered by feeding needs both during the day and night (Davis et al., 2004). At around 10-12 weeks of age, night-time sleep is facilitated, and sleep fragmentation decreases as circadian rhythms start to mature (Mirmiran et al., 2003) and the ability to retain calories increases (Bathory & Tomopoulos 2017).

The phenomenology of sleep in newborns is described by two individual behavioral states known as quiet sleep (QS) and active sleep (AS) (Prechtl, 1974). QS resembles non-rapid eye movement (NREM) sleep and is characterized by restricted gross body movements (excluding brief startles), regular rhythmic respiration, lack of eye movements and slow waves on the EEG (Korotchikova et al., 2016). Correspondingly, AS is similar to rapid eye movement (REM) sleep and is characterized by irregular breathing patterns, increased heart rate (HR), eye movements, twitches, gross body movements and lower amplitude EEG patterns (Grigg-Damberger, 2016). A third sleep state known

as indeterminate or transitional sleep includes traits of both AS and QS. By 4-8 weeks of age, deep sleep is no longer called QS because sleep spindles associated with adult NREM are visible on the EEG, and by 6 months of age, high-amplitude slow wave spikes characteristic for the deepest stages of adult NREM sleep appear in the EEG (Mindell et al., 1999; Galland et al., 2012b). Overall, sleep changes developmentally: sleep intervals are lengthened, QS and NREM sleep increases, AS and REM sleep decreases and the time spent in transitional sleep also declines with age (Anders & Keener 1985; Ficca et al., 2000).

1.2 The Effects of Infant Sleep Disturbances

It is normal for infants to awaken briefly between sleep cycles during the night (Anders, 1978), and for the ones with the capacity to fall back asleep without parental help (i.e. self-soothers), these nocturnal awakenings appear to be harmless (Goodlin-Jones et al., 2001; Weinraub et al., 2012). However, recurrent night awakenings in infancy may lead to overall reduced sleep duration, disturbances to circadian rhythms and pathological fragmented sleep (Mäkelä et al., 2018). Moreover, night awakenings in early infancy, especially in non-self-soothers, are one of the most often reported concerns of parents when asked to evaluate the quality of their infant's sleep (Palmstierna et al., 2008). Though sleep is considered having a pivotal role in the rapid brain development that occurs during the early years of life (Dahl, 1996), not many longitudinal studies have focused on assessing the long-term effects of night awakenings in early infancy (Palmstierna et al., 2008). Therefore, increasing importance has been given to understanding the consequences of sleep disturbances on the physiological and cognitive development of infants. Numerous infant sleep questionnaire-based studies have been carried out to analyze associations between distinctive sleep characteristics and general cognitive functioning, with no such correlations observed in most cases (Spruyt et al., 2008; Bernier et al., 2010; Mindell & Lee 2015; Mäkelä et al., 2018). Yet, in an example of a study that used actigraphy to assess infant sleep, a negative correlation between increased motor function or nocturnal awakening and cognitive functioning in 10-month-old healthy infants was observed (Scher, 2005). Notably, in comparison to study methods in which physiological measures are considered, questionnaire-based studies rely solely on the participation and memory recall of exhausted parents. Consequently, the varying outcomes of both questionnaire- and actigraphy-based research methods have led to inconsistent results, thus, a

consensus of the association between sleep and psychomotor, cognitive and temperament developmental effects has not been established (Douglas & Hill 2013; Field, 2017).

1.3 Tools for Monitoring Infant Sleep

There are a variety of tools available to evaluate sleep in infants, though these approaches tend to be more quantitative than qualitative (Isler et al., 2016), and the most reliable methods are the most intrusive ones (Barbeau & Weiss 2017). Historically, the preferred infant sleep evaluation technique has been direct behavioral observation (Prechtl, 1974). However, sleep state classification based on behavioral observation is laborious, requires special training and is commonly limited to a couple of hours during the daytime (Sadeh, 2015). Presently, the golden standard for sleep evaluation is polysomnography (PSG), which is a multi-parametric test used to record the activity of different physiological factors such as respiration, EEG, ECG, EMG and EOG. However, PSG recordings require sophisticated equipment, trained experts and dedicated sleep laboratory setups (Grigg-Damberger, 2016). Furthermore, subjects are required to endure the application of multiple sensors and electrodes in addition to sleeping in an unnatural and disturbing environment. This creates a challenge to studying natural sleep patterns and is a key weakness of PSG recordings (Mouthon & Huber 2015). Therefore, a sleep monitoring technique that requires minimal expertise to interpret and that can be used comfortably for longer time periods in the natural home environment is needed.

Alternatively, actigraphy has been explored as a methodology to assess infant sleep-wake patterns (Sadeh et al., 1995; So et al., 2005) for its cost-effectiveness and non-intrusiveness. In actigraphy, a miniaturized acceleration sensor is used to measure physical motion, and sleep-wake classification algorithms are employed to differentiate wake from sleep (Sadeh et al., 1995; Galland et al., 2012a). Though actigraphy has presented relatively good agreement rates (89%-94%) with PSG sleep-wake identification predictors in infants up to 6-months-of-age, it has the disadvantage of measuring only limb activity, hence actigraphy provides no direct information on sleep state related behavior, such as respiration (So et al., 2005). Moreover, actigraphy for infant sleep monitoring purposes lacks standardized protocols in terms of utilization and interpretation of data, resulting in high variability of sleep-wake pattern estimation and is therefore not used in routine practice (Meltzer et al., 2012).

1.4 Respiration and HR as Measures Used for Sleep Stage Classification

To advance sleep state scoring in infants, several methods that require only a portion of prevailing PSG measures have been investigated (Harper et al., 1987; Myers et al., 1997). Cardiorespiratory studies are standard procedures for monitoring the health status of patients in the neonatal intensive care unit (Zhu et al., 2015), and because they are easy to perform in varying environments, the compilation of good quality cardiorespiratory signals in comparison to other PSG signals is facilitated (Southall et al., 1983). Moreover, it is known that cardiorespiratory rates vary between different sleep states and are commonly lower during sleep compared to awake (Heimann et al., 2013, Barbeau & Weiss 2017). During REM sleep the effects of an increased sympathetic tone and activation of behavioral brain areas result in increased HR (Chouchou & Desseilles 2014). In contrast, NREM sleep is characterized by a dominant parasympathetic vagal tone, which results in a lowered HR and respiratory sinus arrhythmia (RSA). RSA is described by a reduction in HR during inspiration and an increase in HR during expiration (Yasuma & Hayano 2004). Although HR has the potential to serve as a parameter for sleep state differentiation in infants (Werth et al., 2017), it requires further software interpretation of the output and is not currently used regularly for bedside sleep monitoring (Barbeau & Weiss 2017). Respectively, the use of respiratory rate (RR) for sleep classification purposes has been justified in various studies. For example, breath intervals have been shown to naturally vary between infant REM and NREM sleep (Terrill. et al., 2012). Moreover, Harper et al. (1987) found that variation in RR was distinctly the best parameter for infant sleep state classification. In addition, Terrill et al. (2012) concluded that by quantifying the nonlinear property of respiration alone, it is possible to classify sleep states in comparison to PSG with an 80% agreement rate.

1.5 Wearable Sensor Technology for Infant Sleep Monitoring

Constant health monitoring has received great attention, as a selection of wearable sensors and devices comprising triaxial microelectromechanical systems (MEMS) sensors, smart fabrics and wireless communication networks (Chan et al., 2012) have been developed. For example, various wearable prototypes have been manufactured for early detection of life-threatening events in neonates and infants (Linti et al., 2006; Cao et al., 2007; Rimet et al., 2007; Bouwstra et al., 2009). With increasing significance to develop automatic sleep state coding techniques, wearable motion-sensing technology has sparked interest in the field of infant sleep development research for its

convenience and practicality to monitor long-term activity without disturbances (Zhu et al., 2015; Chan et al., 2012). In addition to sleep stage classification, wearable sensors have the potential to detect movement (Chen et al., 2016) and respiratory disorders (Zhu et al., 2015). Overall, wearable sensor technology may bring added value to clinical sleep studies by providing additional information on sleep quality and cyclicity, and more reliability in comparison to parental sleep diaries. However, given that the technology of wearable sensors is relatively new and that there are no standard protocols for data interpretation, further studies are required for clinical study validation purposes.

1.6 Current Study

The aims of the current study were to compare signals retrieved by a wearable motion sensor (Movesense sensor (MS) by Suunto) and integrated textile electrodes to the outputs of the standardly used respiratory piezo effort (RESP) belt and stick-on ECG electrodes during daytime EEG recordings conducted on newborns and infants. Moreover, the feasibility of the MS's overnight home-use was assessed to determine whether good quality respiration and ECG data could be collected for future sleep-wake classification.

2. Material & Methods

2.1 Ethical Approval

The study was approved by the Helsinki University Hospital Ethics Committee for gynecology, obstetrics, pediatrics and psychiatry. All subjects were volunteers recruited from the maternity ward of Helsinki University Women's Hospital or through an application form available on Baby Brain Activity (BABA) Research Center's website (http://www.babacenter.fi/our-projects/participate/). Parents were asked to provide a written informed consent prior to study initiation, and no monetary incentive was provided for participation.

2.2. Participants

2.2.1 Part 1: EEG Respiratory Belt versus MS

The study population (N=10) consisted of four (3 female, 1 male) healthy term infants (41-42 weeks old), three male term infants with mild asphyxia (41-42 weeks old), one male preterm infant (42 weeks old by the time of the study) and two female healthy 3-month-old infants (52-53 weeks old).

2.2.2 Part 2: Overnight MS Home Recordings

All study subjects (N=9) were healthy term infants (4 males, 5 females) aged 3-6 months.

2.3 Recording Methods

In part 1 of the study, MS and EEG recordings were conducted simultaneously during the daytime for a period of 1-2 hours. The recordings were performed in dim lighting and constant room temperature conditions. In part 2, test subjects were provided with a MS and smartphone to take home for 1-2 nights (total recording time 8-14 hours/night).

2.3.1 EEG Recording

EEG studies were carried out at BABA Center Helsinki University Children's Hospital with Eego EEG & EMG recording Software (LE-200 Eego, Ant Neuro) and at the clinical neurophysiological unit with the NicoletOne EEG system (Natus) of the Helsinki University Children's Hospital. An EEG cap (Waveguard^{TM}, Ant Neuro) was used to record brain electrical activity and disposable electrodes (BlueSensor NF, Ambu) were used to record physiological variables (e.g. ECG, EOG and submental EMG). Respiration was recorded with the RESP belt (Piezo effort, Pro-Tech), which measured changes in strain caused by abdominal breathing movements. The EEG accessories were placed on each infant during feeding, and, when somnolent, the infant was carefully adjusted into a supine position on the mother's lap to minimize EEG signal interference. Sleep states were classified into QS, AS and indeterminate sleep using EEG, behavioral, EOG and breathing pattern criteria (Anders et al., 1971).

2.3.2 MS Recording

A custom-made wearable cover garment (i.e. "actidiaper") was manufactured with the cooperation of Aalto University (Dr. Elina Ilén, Fashion/Textile Futures research team) to measure abdominal respiration with the MS (Figure 1). The MS was clipped onto the mid-frontal panel of the actidiaper's waistband, and two fleece or silver-coated textile electrodes, located on the backside of the waistband, were used to record ECG activity (Figure 1). The actidiaper was placed over the child's disposable diaper, so that the ECG textile electrodes had direct skin contact. The MS's ECG, accelerometer (ACC), gyroscope (GYRO) and magnetometer (MAGN) channels were all tested in part 1 of the study (RESP belt versus MS). However, in part 2 (MS home recordings), the MAGN channel was disabled.

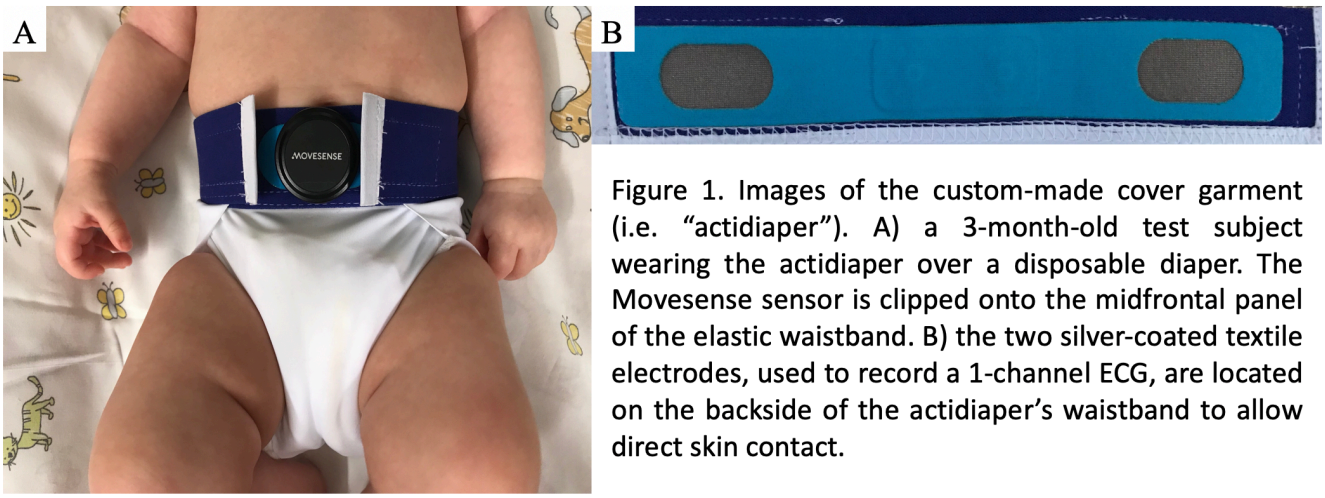

Figure 1. Images of the custom-made cover garment (i.e. "actidiaper"). A) a 3-month-old test subject wearing the actidiaper over a disposable diaper. The Movesense sensor is clipped onto the midfrontal panel of the elastic waistband. B) the two silver-coated textile electrodes, used to record a 1-channel ECG, are located on the backside of the actidiaper's waistband to allow direct skin contact.

2.4 Presentation of MS Technology

In 2017, the Finnish company Suunto released Movesense, a programmable sensor along with an open Representational State Transfer Application Programming Interface (REST API), designed for wireless motion-sensing mobile application developers. The MS includes a sensor module (LSM6DS3, STMicroelectronics) that contains three microelectromechanical systems (MEMS) sensors for recording different types of movement. Each MEMS sensor has three measurement channels for recording movement in X, Y and Z axes (Figure 2). The MEMS sensors included in the MS are the ACC, GYRO and MAGN. Additionally, the MS contains channels for recording temperature and a 1-channel ECG (Movesense data sheet 2017). Table 1 contains a list of the measuring units, functional ranges and sampling rates of the MS's MEMs sensors. The sampling rates used in the current study are also presented in Table 1.

The MS functions via a nRF52832-microcircuit (Nordisk Semiconductor) that includes a 32-bit M4-processor (ARM Cortex) in addition to FLASH (512 kB) and RAM (64 kB) memory for running the Movesense software and applications. It uses a small internal memory (3 Mb) for temporary data storage and Bluetooth Low Energy 4.0 (BLE) to transfer data to a smartphone. The MS is powered with a CR 2025 Lithium coin cell battery (Movesense data sheet 2017). Its small size and light weight (10 grams with the battery included) makes it easy to use and wear, thus enabling the MS to be used for neonate and infant sleep monitoring.

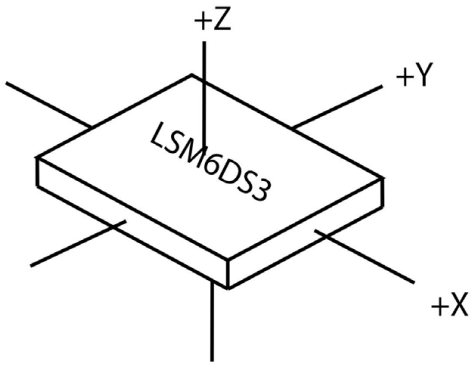

Figure 2. An illustration of the MS module (LSM6DS3) with corresponding measurement axes coordinates (Movesense data sheet 2017).

Table 1. Technical specifications of Movesense MEMS sensors (Movesense data sheet 2017).

Sensor	Measuring Unit	Functional Range	Sampling Rates (Hz)	Study Sampling Rate (Hz) **
ACC	Linear acceleration: (g = 9,81 m/s^2)	±2, ±4, ±8, ±16	12.5, 26, 52, 104, 208	12.5
GYRO	Angular velocity: (°/s = degree per second)	±125, ±245, ±500, ±1000, ±2000	12.5, 26, 52, 104, 208	12.5
MAGN	Magnetic flux density: gauss = (100 micro tesla (μT)	±4, ±8, ±12, ±16	12.5, 26, 52, 104, 208	12.5

ACC = Accelerometer, GYRO = Gyroscope, MAGN = Magnetometer, MEMS = Microelectromechanical systems
** Sampling rates used in the current study

2.4.1 SleepSense Mobile Application

Data measured with the MS was collected with a mobile application (SleepSense) developed in-house for Android operating system (see Figure 3). The data was transferred via BLE 4.0 to a smartphone (Nokia 5) and the SleepSense application was used to save it (in text file format) into a Google Drive account. Each BLE package or file that arrived in the smartphone was given a timestamp based on the internal clocks of the smartphone (i.e. system time) and the MS (i.e. measurement time). With SleepSense, the desired MEMS sensors could be selected, and the sampling rates adjusted. In addition, the application had the online option for inserting annotations (e.g. “cry”, “sleep”, “move”, “suck”, “free text”) during the recording time to facilitate further analysis.

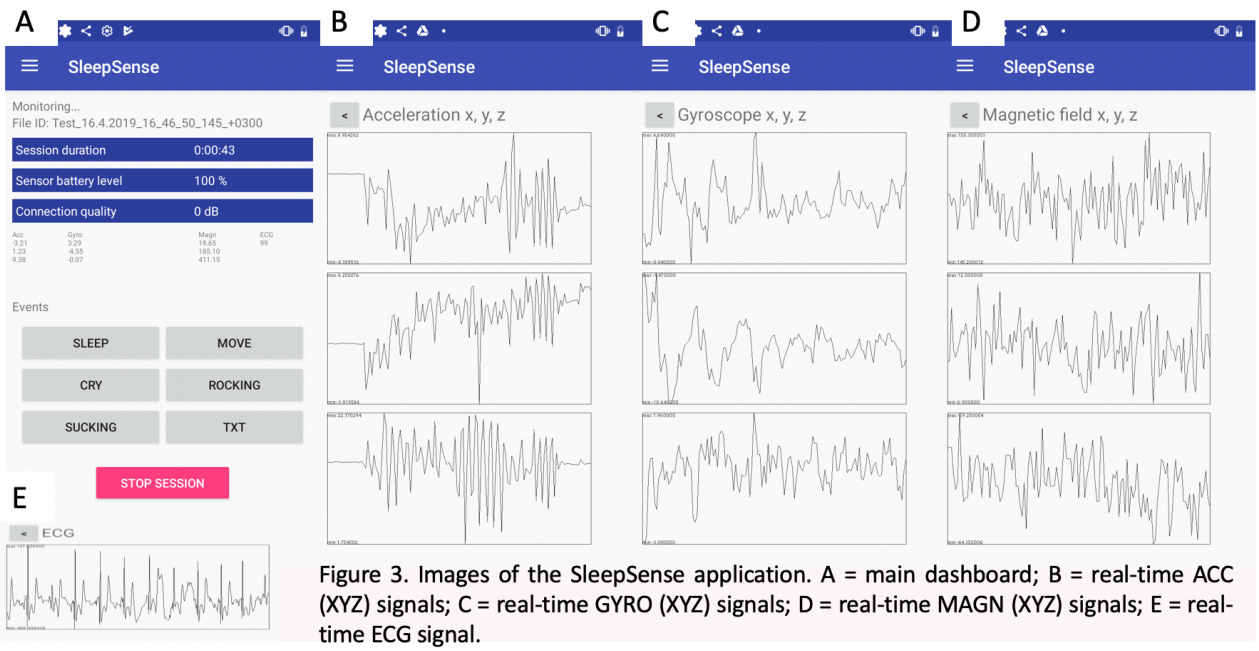

Figure 3. Images of the SleepSense application. A = main dashboard; B = real-time ACC (XYZ) signals; C = real-time GYRO (XYZ) signals; D = real-time MAGN (XYZ) signals; E = real-time ECG signal.

2.5 Signal Processing

RESP belt and MS respiratory and ECG signals were preprocessed and edited in MATLAB (R2018a) to extract relevant information from the raw data and to allow signal comparisons. The raw data was digitally filtered and synchronized based on measurement time and sampling frequency.

2.5.1 Filtering the Signals

The time lag between the EEG software and the MS was determined by locating an artifact visible on the outputs of both measurement devices. EEG recorded RESP and ECG signals were then time synchronized with MS recorded data, and artifact-free (i.e. detectable respiratory signal) epochs were manually selected from the outputs of both devices. To extract frequencies relevant to respiration, the selected epochs (over or equal to 30 seconds each) were digitally band-pass filtered (high-pass cut-off point = 0.1 Hz; low-pass cut-off point = 2 Hz) with the Butterworth filter and the filtfilt-function in MATLAB.

2.5.2 Sampling Frequency Synchronization

For an easier comparison of signals from different devices, we used MATLAB's resample-function to resample the signals: the RESP signal was resampled from 500/2000 Hz to 12.5 Hz, and the ECG signal was resampled from 500/2000 Hz to 125 Hz.

2.6 Data Analysis

The following signal comparison variables were used to quantify the RR detection efficacy of the MS in comparison with the RESP belt: RR (breaths/minute), phase locking value (PLV) and signal-to-noise ratio (SNR) value (dB). First, power spectrum was calculated to determine dominant RR in each signal. Next, the SNR value of each signal was quantified to determine the relative specificity of the given signal in reflecting respiration. This was followed by the calculation of dominant delta RRs and delta SNR values to assess measurement agreement between the measurement devices. Finally, PLVs were calculated to analyze the level of phase synchrony between RESP and MS signals, and surrogate testing was used for assessing statistical significance. Figure 4 shows a schematic structure of the respiratory signal analysis pipeline.

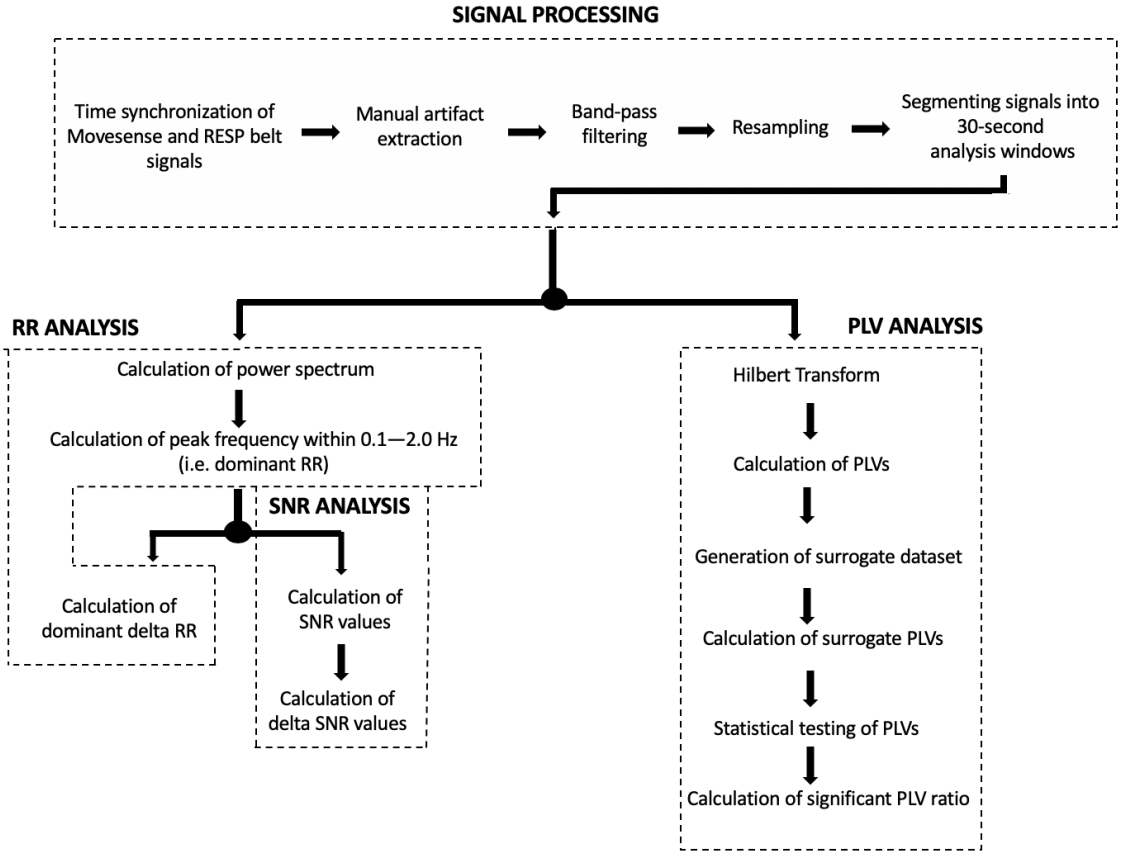

Figure 4. A schematic illustration of the respiratory signal analysis pipeline. Starting with signal processing and proceeding onto RR and SNR analysis, and PLV analysis steps. The black circles indicate points of intersection.

2.6.1 RR Analysis

The artifact-free, time synchronized, and resampled epochs were segmented into 30-second epochs, power spectrum was computed using MATLAB's pwelch-function and the peak frequency

within 0.1—2.0 Hz was taken as the representative of dominant RR for each epoch. To calculate the dominant delta RR between RESP and MS, the dominant RR detected by each MS channel and axis was subtracted one at a time from the dominant RR detected by the RESP belt.

2.6.2 PLV Analysis

Each periodic biosignal has a phase that changes over time. The synchrony between two signals can be determined by calculating the absolute value of the mean phase difference (i.e. the PLV). In other words, PLVs are complex unit-length vectors used to measure the phase interaction between two signals (Mormann et al., 2000). However, complex values are not informative as such, thus PLVs are usually normalized to values ranging from 0 to 1. If the phases of the two signals are strongly coupled, the phase difference remains stable and the PLV approaches the value 1. In contrast, if the phases of the two signals are independent of each other, the phase difference increases and the PLV is closer to 0 (Tokariev et al., 2012).

2.6.2.1 Calculating and Statistically Testing the PLV

To evaluate phase synchrony with PLVs, the procedure described elsewhere (Lachaux et al.,1999; Lauchaux et al., 2000; Tokariev et al., 2012) was followed. In summary, the Hilbert Transform (Tass et al., 1998) was used to convert the original signals into complex vector values (i.e. analytical signals). These were then used to calculate the PLVs for 30-second analysis windows. Next, a surrogate dataset was generated to assess the stability of phase difference between signal pairs (Hurtado et al., 2004). As in Pakkala's (2018) study, 1.5-second-long segments of the original signals were used to generate surrogate 30-second analysis windows. Finally, PLVs were calculated for the surrogate signals, and compared to original PLVs. If the original PLV was greater than 99% of the surrogate PLVs, the epoch's PLV was determined to be statistically significant ($p < 0.01$) (Lachaux et al., 2000).

2.6.2.3 Analysis of PLV Significance

The percentages of significant PLVs were calculated for each test subject's measurement channel and axis individually with the following equation (Eq. 1):

$$\frac{number\ of\ significant\ PLVs}{All\ PLVS} \times 100 \quad (1)$$

2.6.3 SNR Analysis

The SNR of a signal is determined by calculating the ratio of signal power over noise power. The higher the SNR value, the better the signal. To calculate the SNR of each 30-second epoch, the areas of the dominant RRs and the frequency areas surrounding them (+/- 0.1 Hz) were assigned to the signal power. Respectively, the frequency areas excluded from this range were assigned to the noise power. SNR values were calculated with (Eq. 2), and delta SNR values were calculated in the same way as the dominant delta RRs (see 2.6.1 RR Analysis).

$$(2) \qquad SNR\ (dB)\ =\ 10\ log_{10}\left(\frac{P_{signal}}{P_{noise}}\right)$$

2.6.4 Heart Rate Variability (HRV) Analysis

The outputs of the reference ECG and the MS's ECG were converted into EDF format and time synchronized with MATLAB. Both ECG signals were simultaneously processed with Kubios HRV Premium. First, artifact correction was performed using the setting "very strong threshold", followed by selection of 10-minute HRV analysis windows. The following HRV parameters were then calculated for the selected analysis window of each test subject individually (N=9): mean HR (beats/minute), root mean square of successive differences (RMSSD) (milliseconds (ms)) between heart beat intervals and high frequency (HF) power (ms^2). Mean HR and RMSSD are time-domain HRV parameters used to quantify the amount of variability between successive heart beats. Correspondingly, HF power represents a frequency-domain HRV parameter that is used to estimate the absolute power (i.e. signal energy) of the HF band (0.15 – 0.4 Hz), also known as the respiratory band because it is influenced by RR (Shaffer and Ginsberg 2017). In the current study however, the HF band's upper limit was set at 0.5 Hz to represent neonate and infant RRs (de Beer et al., 2004; Ranta 2018).

2.7 Statistical Methods

Statistical analyses were performed with SPSS software package version 25.0 and MATLAB (2018a). All tests were two-tailed and the threshold for statistical significance was set at $p < 0.05$.

2.7.1 Statistical Analysis of Respiratory Signal Comparison Variables

The dominant delta RRs, PLVs and delta SNR values, calculated for every 30-second epoch of each measurement channel, were combined to obtain individual (per study subject) averages for all three

respiratory signal comparison variables. Boxplots and scatterplots confirmed that the dispersion of each signal comparison variable was non-normally distributed, and therefore non-parametric statistical tests were used to establish which one of the MS's measurement channels (independent variables) was the best at detecting respiration. ANOVA comparison (Kruskal-Wallis test) was used to conclude whether there were statistically significant differences between the dependent variables (i.e. dominant delta RR, PLV, delta SNR value) and the independent variables (i.e. the axes (XYZ) of the MS's measurement channels). If the Kruskal-Wallis test provided a significant result, pair-wise comparisons were conducted, using the independent t-test (Mann-Whitney U), to determine in between which two axis pairs (i.e. XY, XZ, YZ) the statistically significant difference was present. Corrections for multiple Post-hoc testing, such as Bonferroni correction, were not used because the purpose of the study was exploratory (Streiner & Norman 2011) and the number of outcomes was small (i.e. dominant delta RR, delta SNR value and PLV) (Schulz & Grimes 2005).

2.7.2 Statistical Analysis of ECG Signal Parameters

Individual averages were used to calculate HRV parameter (i.e. mean HR, RMSSD, HF power) grand averages (over study subject) for both reference and MS ECG signals separately. These grand averages were then used to calculate combined HRV parameter means and mean differences (i.e. reference mean HRV parameter – MS mean HRV parameter). A one sample T-test was used to confirm that the mean differences of both measurement devices had no significant difference between each other. Moreover, the combined HRV parameter means were used in a linear regression test to verify the level of agreement between both measurement techniques. Bland-Altman and linear correlation graphs were drawn for each HRV parameter separately to visualize agreement rates between the reference and MS ECG outputs.

2.8 Overnight Home-Recorded Data Analysis

The raw data measured by the MS (ACC (XYZ), GYRO (XYZ) and ECG) was visualized in MATLAB (R2018a). Total recording times per night were calculated for each test subject, and the following statistics were computed for the outputs of ECG and GYRO measurement channels: readable respiration (GYRO) and ECG signals; noise; and technical failures (all expressed as percentages).

2.8.1 Actidiaper User Experience Questionnaires

Parental acceptance of the actidiaper and overall user experience was assessed by interviewing the parents of the study subjects (N=6). Questionnaires were handed out to the parents and the replies were acquired via email and telephone. In the questionnaire, we asked parents to provide feedback on dressing and wearing the actidiaper, effects of actidiaper usage on night-time feedings and/or diaper change, level of comfort and easiness to use, and materials used on the product. Moreover, the parents could express their views on how to improve and facilitate usage of the actidiaper and SleepSense application.

3. Results

3.1 Selection of Data

In part 1, respiratory and ECG signals were recorded from all 10 participants with both reference (RESP belt and disposable stick-on ECG electrodes) and MS (ACC, GYRO, MAGN and ECG channels) measurement parameters with a total duration of 11 hours. One test subject was excluded from the HRV analysis (N=9) because the MS ECG signal was artifactual (see Supplementary Material). In part 2, overnight home recorded data was collected from 9 study subjects with the MS's ACC, GYRO and ECG channels. However, the ECG's of two study subjects were not available, and in the case of one study subject, the ECG signal was only noise and was therefore excluded from the visual analysis. In total, approximately 138 hours of data was obtained.

3.2 Part 1: Detection of RR

A total of 499 epochs (30 seconds/epoch: total = 4.2 hours (38% of collected data)) consisting of good quality respiratory signals (EEG RESP channel output and MS channel outputs (ACC, GYRO, MAGN)) were selected for further analyses (see Supplementary Material for illustration of selection criteria).

ANOVA comparisons (Kruskal-Wallis) revealed significant differences for each respiratory signal comparison variable (dominant delta RR: $\mathcal{X}_2^2$ = 16.6, p = 0.03, *total df* = 89 ; PLV: $\mathcal{X}_2^2$ = 53.3, p = 9.63E-09, *total df* = 89; delta SNR value: $\mathcal{X}_2^2$ = 39.8, p = 3.53E-06, *total df* = 89) , and a total of 36 channel axis pairwise comparisons (Mann-Whitney U) confirmed that these differences were

present between the axis pairs summarized in Table 2 and Figure 5. Based on these results, we concluded that the MAGN measured RR most inaccurately, whereas, the GYRO mimicked the RESP belt's RR detection levels the closest, and so it was also considered to be a more accurate RR detector than the ACC. To support this claim, the GYRO's Y channel RR detection accuracy was significantly better than the RR detection accuracy of all ACC channels. In addition, the GYRO's X channel measured RR more precisely than the ACC's X channel, and nearly better than the ACC's Y channel (P = 0.07, Z = -1.81). Notably, no outliers were detected among the GYRO's Y channel dominant delta RRs (see Figure 5). However, an outlier which is likely explained by noise, was detected among all other MS channels (except MAGN X and Z). Likewise, an outlier explained by excessive noise, was detected among the delta SNR values of the GYRO Y and MAGN Z channels. Conversely, the outlier observed among the recorded dominant RRs of the ACC X channel (see Figure 6) is explained by a good signal to noise ratio.

In conclusion, the GYRO's Y channel was the most accurate RR detector (mean dominant delta RR: -1.8 breaths/minute) (see Figure 5 and 6), stability of phase synchrony was greatest between RESP belt and GYRO X (mean PLV: 0.73; mean ratio of significant PLVs: 92.1%) and Y signals (mean PLV: 0.73; mean ratio of significant PLVs: 92.6%) (see Figure 5 and 7), and the SNR values calculated from the GYRO's X (mean delta SNR value: 3.27 dB) and Y (mean delta SNR value: 3.11 dB) channels matched RESP belt SNR values (see Figure 5 and 6) the closest.

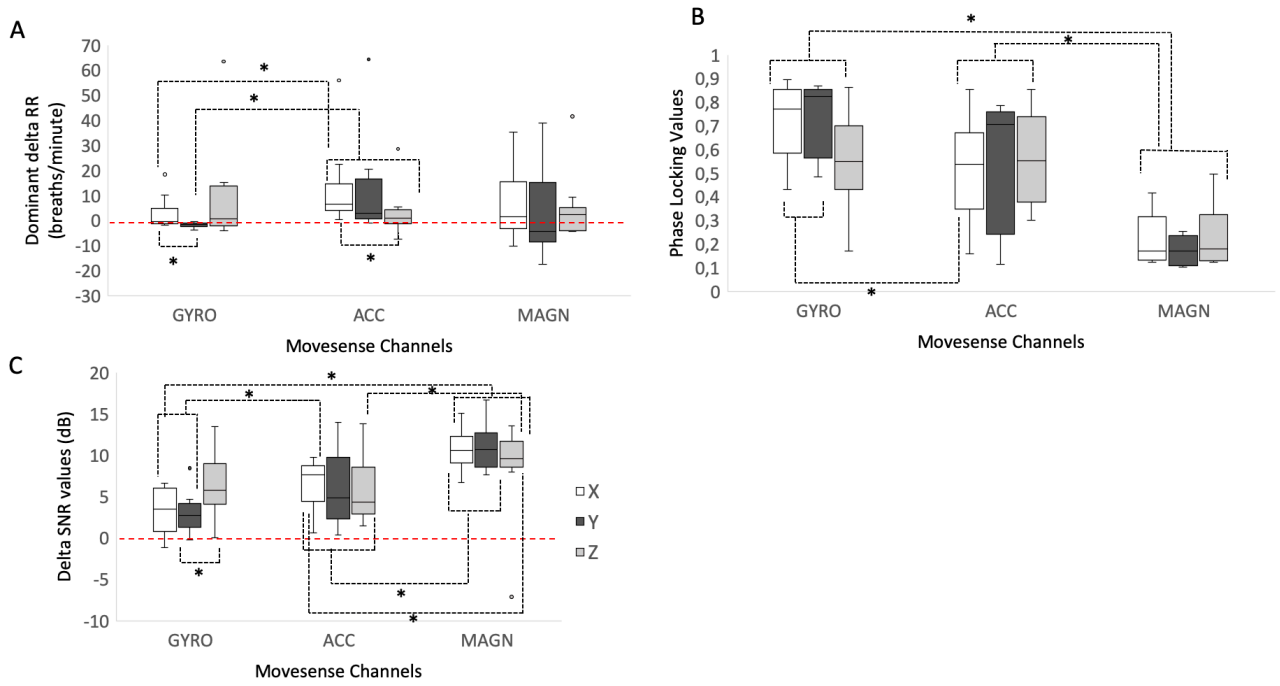

Figure 5. Data dispersion of the (per study subject, N=10) individual averages of respiratory signal comparison variables. A) differences between RESP belt detected dominant RRs and MS channel detected dominant RRs (i.e. dominant delta RRs (breaths/minute)), B) calculated PLVs for all MS channels and C) differences between SNR values (dB) calculated from the RESP belt and the MS channel outputs (i.e. delta SNR values). Small dominant delta RRs and delta SNR values indicate strong correlations with RESP belt RR detection levels and SNR values, and PLVs equal to or close to 1 imply strong phase synchrony between reference and test signals. The medians are indicated by the horizontal lines within the boxes, the 25th- and 75th- percentiles are denoted by the boundaries of the boxes, the highest and lowest values are indicated by the whiskers, and outliers are denoted by individual data points. The red dotted lines in graphs A and C denote target levels (where delta is equal to zero). Significant ($P < 0.05$) differences between axis pairs are presented with dotted brackets and black asterisks. The legend in graph C includes the color codes for MS channel axes.

Table 2. A summary of the significant ($p < 0.05$) axis pairwise comparisons among average dominant delta RRs, PLVs and delta SNR values of all study subject individual averages (N=10).

PLV Channel Pairs	Statistics	Delta SNR value Channel Pairs	Statistics	Dominant delta RR Channel Pairs	Statistics
ACC Z MAGN Y	*P* = 1.83E-04; *Z* = 3.74	GYRO X MAGN X	*P* = 1.83E-04; *Z* = -3.74	ACC X GYRO Y	*P* = 1.83E-04; *Z* = 3.74
GYRO X MAGN X	*P* = 1.83E-04; *Z* = 3.74	GYRO X MAGN Y	*P* = 1.83E-04; *Z* = -3.74	ACC Y GYRO Y	*P* = 5.04E-04; *Z* = 3.48
GYRO X MAGN Y	*P* = 1.83E-04; *Z* = 3.74	GYRO Y MAGN X	*P* = 2.46E-04; *Z* = -3.67	ACC X GYRO X	*P* = 0.01; *Z* = 2.46
GYRO Y MAGN X	*P* = 1.83E-04; *Z* = 3.74	GYRO Y MAGN Y	*P* = 3.30E-04; *Z* = -3.59	ACC X ACC Z	*P* = 0.02; *Z* = 2.31
GYRO Y MAGN Y	*P* = 1.83E-04; *Z* = 3.74	ACC X MAGN Y	*P* = 2.83E-03; *Z* = -2.99	GYRO X GYRO Y	*P* = 0.02; *Z* = 2.31
GYRO X MAGN Z	*P* = 2.46E-04; *Z* = 3.67	GYRO X MAGN Z	*P* = 2.83E-03; *Z* = -2.99	ACC Z GYRO Y	*P* = 0.02; *Z* = 2.27
GYRO Y MAGN Z	*P* = 2.46E-04; *Z* = 3.67	ACC X MAGN X	*P* = 3.61E-03; *Z* = -2.91		
ACC Z MAGN X	*P* = 7.69E-04; *Z* = 3.36	GYRO Y MAGN Z	*P* = 3.61E-03; *Z* = -2.91		
ACC Z MAGN Z	*P* = 7.69E-04; *Z* = 3.36	ACC Z MAGN X	*P* = 5.80E-03; *Z* = -2.76		
GYRO Z MAGN Y	*P* = 7.69E-04; *Z* = 3.36	ACC Z MAGN Y	*P* = 5.80E-03; *Z* = -2.76		
ACC X MAGN Y	*P* = 1.01E-03; *Z* = 3.29	GYRO Z MAGN Y	*P* = 0.01; *Z* = -2.46		
GYRO Z MAGN X	*P* = 1.31E-03; *Z* = 3.21	ACC X GYRO Y	*P* = 0.02; *Z* = 2.38		
GYRO Z MAGN Z	*P* = 1.31E-03; *Z* = 3.21	ACC X MAGN Z	*P* = 0.02; *Z* = -2.38		
ACC X MAGN X	*P* = 2.83E-03; *Z* = 2.99	ACC Y MAGN X	*P* = 0.02; *Z* = -2.38		
ACC X MAGN Z	*P* = 3.61E-03; *Z* = 2.91	ACC Y MAGN Y	*P* = 0.02; *Z* = -2.38		
ACC Y MAGN Y	*P* = 4.59E-03; *Z* = 2.83	GYRO Z MAGN X	*P* = 0.02; *Z* = -2.30		
ACC Y MAGN X	*P* = 0.01; *Z* = 2.46	ACC X GYRO X	*P* = 0.03; *Z* = 2.23		
ACC Y MAGN Z	*P* = 0.01; *Z* = -2.46	GYRO Y GYRO Z	*P* = 0.03; *Z* = -2.15		
ACC X GYRO X	*P* = 0.02; *Z* = 2.30	ACC Z MAGN Z	*P* = 0.04; *Z* = -2.01		
ACC X GYRO Y	*P* = 0.03; *Z* = -2.15				

ACC = accelerometer; GYRO = gyroscope; MAGN = magnetometer
Number of comparisons per signal comparison variable = 36; Post-hoc Mann-Whitney U test

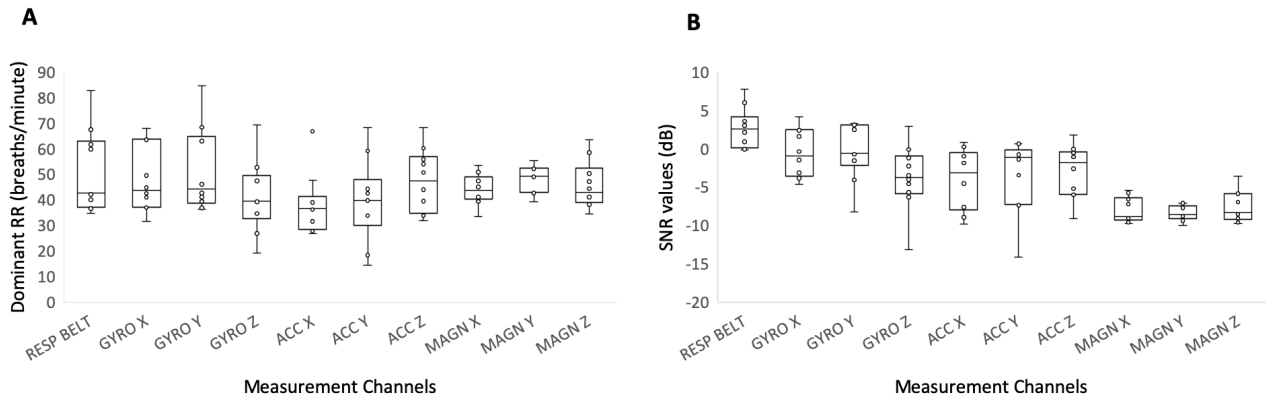

Figure 6. Data dispersion of the individual averages (N=10) of A) dominant RR (breaths/minute) and B) SNR values (dB) calculated from the RESP belt and all MS channel outputs. Proximity to RESP belt dominant RRs indicates RR detection accuracy, whereas proximity to RESP belt SNR values indicates higher agreement levels between the SNR values of reference and test signals. Inner data points included. See Figure 1 for more details.

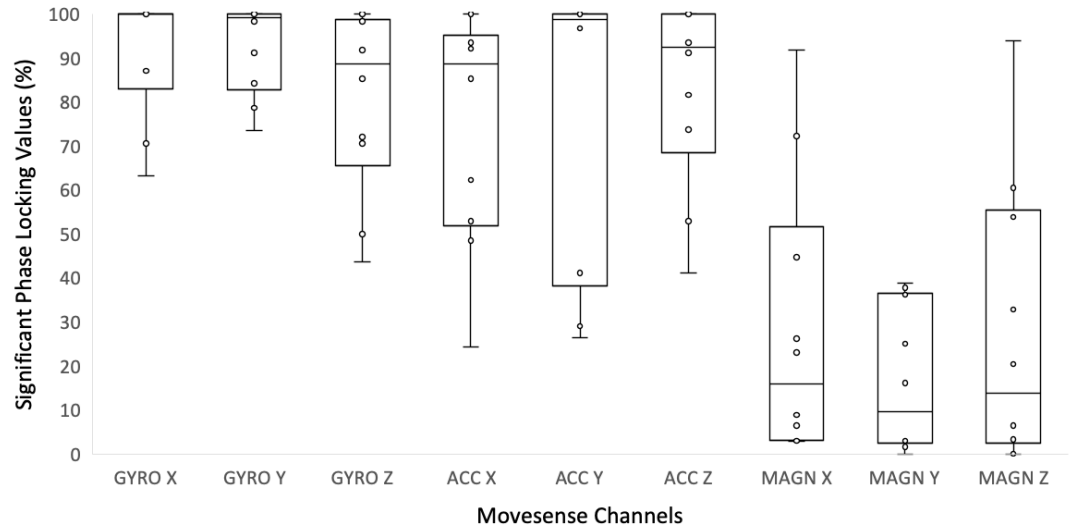

Figure 7. Data distribution of the individual averages (N=10) of significant PLVs (%) among subject specific analysis windows (total N=499). Greater significant PLV ratios indicate more stability in phase synchrony between reference and test signal pairs. Inner data points included. See Figure 1 for more details.

3.3 Part 1: Detection of HR

The MS and reference ECG outputs of nine study subjects were time synchronized and filtered for the HRV analysis (see Material and Methods). A total of 10-minutes of ECG data was selected either from one continuous epoch (N=8) or from several shorter epochs (N=1).

Visual interpretation of both Bland-Altman and linear correlation graphs confirmed a level of agreement between the selected reference and MS ECG analysis windows (see Figure 8). Among the calculated HRV parameters, only three data points (in total) exceeded the lower level of agreements by approximately 0.01 beats/minute (mean HR), 1 ms (RMSSD) and 0.4 ms^2 (HF power). These outliers are likely explained by minor technical errors in R-peak detection. Nevertheless, the

one sample T-test established that the mean differences of the HRV parameters, calculated from the ECG analysis windows of both measurement devices, had no statistically significant difference between each other (mean HR: $P = 0.425$, $df = 8$; RMSSD: $P = 0.295$, $df = 8$, HF Power: $P = 0.338$, $df = 8$). Likewise, the linear regression analysis verified that the means of all three HRV parameters had no statistically significant difference in relation to one another (mean HR: $P = 0.370$, $df = 1$; RMSSD: $P = 0.625$, $df = 1$; HF Power: $P = 0.224$, $df = 1$), further justifying agreement between the measurement devices.

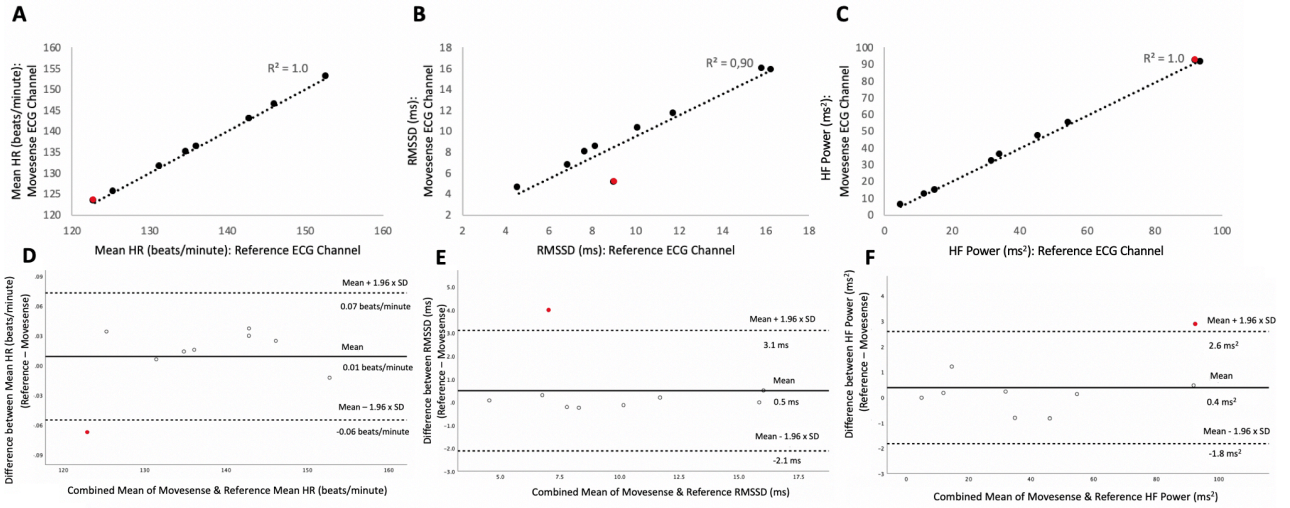

Figure 8. Linear correlation and Bland Altman graphs to compare agreement rates between the HRV parameters calculated from reference and MS ECG analysis windows. The horizontal axes (X) in graphs A-C represent the HRV parameters (i.e. A = Mean HR; B = RMSSD; C =HF power) calculated from the reference ECG signals, and the vertical (Y) axes represent the HRV parameters calculated from the MS ECG signals. The corresponding coefficients of determination (r^2) are also displayed. In graphs D-F, the horizontal (X) axes represent the combined mean values of reference and MS HRV parameters (i.e. D = Mean HR; E = RMSSD; F = HF power), whereas the vertical (Y) axes represent the difference between the corresponding HRV parameters of both ECG outputs (i.e. Reference HRV parameter – MS HRV parameter). The middle horizontal lines denote the mean differences and the dotted lines represent the 95% limits of agreement (mean + 1.96 x SD). The red data points in graphs A-C represent outliers that are equally visible in graphs D-F.

3.4 Part 2: Analysis of Overnight Home Recordings

Due to findings in part 1, the MS's GYRO channel was considered to represent respiration signals in part 2, while the MAGN channels were disabled, and the ACC channel was used to observe general movement activity. The ECG channel was also active in part 2.

3.4.1 Raw Data Assessment

While visually examining the MS's raw data from overnight home recordings (N=9), a cyclic pattern that repeats itself every 1-2 hours (i.e. awake, REM sleep and NREM sleep) could be distinguished from the output of the GYRO channel. Epochs of high activity and movement were considered to represent awake state; epochs with relatively little gross movements and regular breathing patterns were considered to represent NREM sleep; and epochs with irregular respiration signals and occasional brief movements were considered to represent REM sleep (see Figure 9).

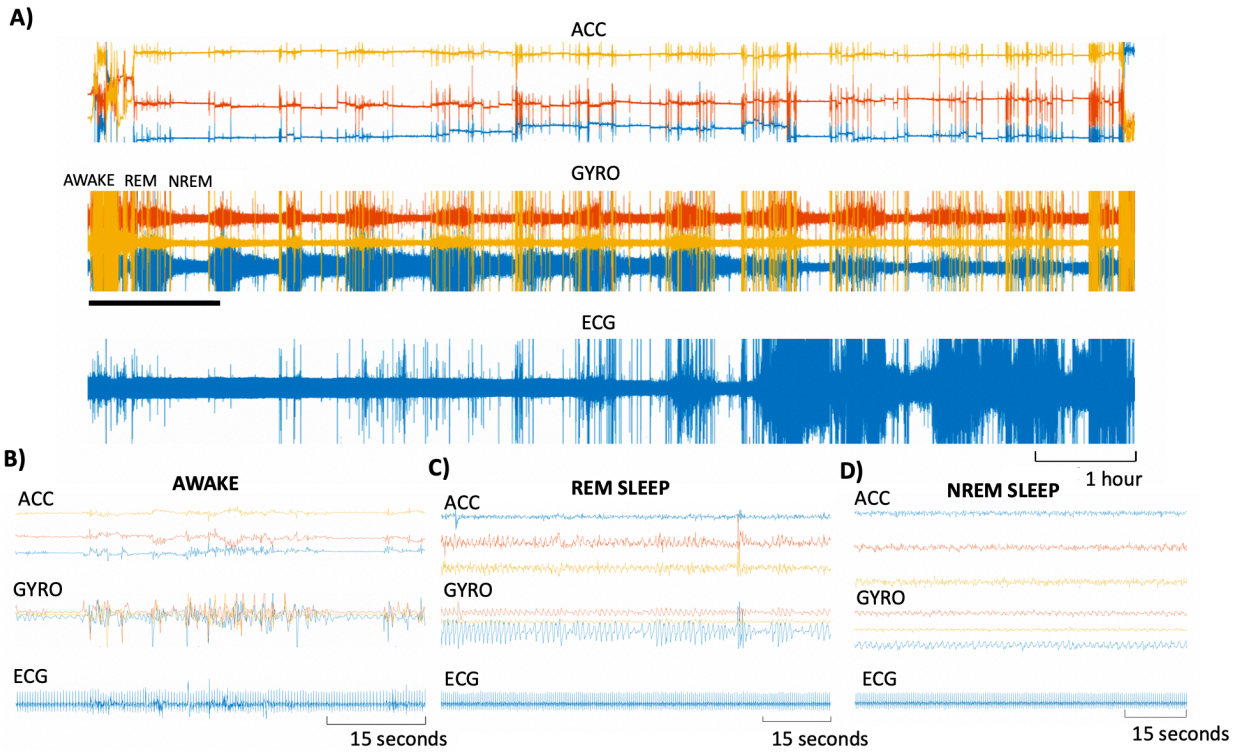

Figure 9. An example of the MS output retrieved from an overnight home recording of one study subject. A) ACC, GYRO and ECG outputs of the full recording (total measurement time: 10.5 hours). The black bar beneath the GYRO signals outlines a segment that contains epochs of awake, REM and NREM sleep states. Magnifications of these states and the corresponding signals are seen in graphs B-D, where B) represents an awake state (gross movement), C) represents REM sleep (brief startle and irregular respiration) and D) represents NREM sleep (relatively still and regular breathing pattern). The vertical axes of each graph represent time (A = hours; B-D = seconds).

3.4.2 Signal Quality Analysis

Two study subjects recorded sleep for two consecutive nights and the rest (N=7) recorded sleep for one night, either continuously or in two parts. A summary of the home recording statistics is presented in Table 3. On average, total recording times lasted for approximately 12.5 hours/night, of which 56.9% represented readable GYRO respiration signal and 40.9% accounted for readable

ECG signal. The remaining 41.8% (GYRO) and 58.1% (ECG) was noise (explained by heavy movement artifacts), and 1.3% (GYRO) and 1.0% (ECG) was technical failure (explained by BLE connection loss).

Table 3. Overnight home recording statistics of all study subjects (N=9).

ID	Number of nights	Total recording time (hh.mm.ss)	Readable (GYRO) respiration signal (%)	Readable ECG signal (%)	GYRO Noise (%)	ECG Noise (%)	Technical failure (GYRO) signal (%)	Technical failure (ECG) signal (%)
1	N1	15.03.37	49.5	13.4	48.9	86.5	1.60	0.09
2	N1	13.11.40	56.4	55.1	43.6	44.8	0	0.12
2	N2	13.07.02	49.6	49.0	48.9	48.4	1.54	2.57
3	N1	14.48.36	45.0	41.4	46.5	53.8	8.55	4.83
4	N1	10.18.11	69.8	76.1	29.8	23.7	0.36	0.25
5	N1	12.12.46	50.9	48.3	49.1	51.7	0	0
6	N1	10.44.42	76.6	46.7	23.3	52.9	0.07	0.39
7	N1	10.29.09	65.9	43.2	34.1	56.6	0	0.30
8	N1	11.17.35	50.7	0.0	48.5	98.9	0.84	1.14
8	N2	13.12.04	56.0	14.7	43.4	84.3	0.62	1.01
9	N1	13.38.40	55.8	62.1	44.2	37.65	0	0.25

Hh= hours, mm = minutes, ss = seconds, N = night

3.4.3 Actidiaper User Experience Questionnaire Results

We collected feedback from the parents of six study subjects to analyze actidiaper user experience from a parental perspective. In general, the mothers of the participants were satisfied with the appearance and the materials, and the actidiaper was regarded as practical and easy to use. One parent was concerned that the actidiaper's waistband may be fastened too tightly, causing discomfort during nocturnal feedings. After overnight use though, all parents felt that the actidiaper had no negative effects on their infant's behavior and/or sleep. However, they had experienced that self-operation of mobile phone data logging software or periodic checking of BLE connection and self-logging of activities during the night was cumbersome.

4. Discussion

4.1 Main Findings

The aim of the present study was to assess the usability of Movesense (a triaxial wearable motion sensor adjusted onto a custom-made actidiaper with integrated textile electrodes) in measuring sleep related RR and HR in newborns and small infants. Comparison of the MS's measurement channel outputs to the (reference) piezo sensor-based RESP belt showed that the GYRO channel's X and Y axes provided the most reliable representation of respiration (when sleeping in a supine position) in comparison to MAGN and ACC channels. Standard HRV parameters showed a high level of agreement between MS and reference ECG signals. However, no matter how tightly the actidiaper's was fastened, whenever the infant was held or moved during the recordings, the waistband was more prone to be displaced. Thus, MS ECG signals were more affected by motion artifacts than reference ECG signals, which is a commonly reported issue with textile electrodes (Patel et al., 2012). Moreover, overnight home recorded data indicated that sleep states could likely be classified based on respiratory (GYRO) signals, and parental acceptance was encouraging for future development of the wearable system.

4.2 Comparison to Related Studies

4.2.1 RR Detection with a MEMS Sensor

While actigraphy only measures limb activity, and provides no information on sleep staging and breathing, it has long been used for sleep/wake state identification (Sadeh, 2015). For example, in a study with a similar setup to ours, Sazonova et al., (2002) reported identifying sleep/wake states with a 72%-92% accuracy based on infant movement and body position data recorded with a triaxial ACC. Though the sensor was directly clipped onto the diaper, respiration was not studied as a key sleep/wake classifier. Nevertheless, cardiorespiratory rates are controlled in a state-dependent manner, and RR-based classifiers have been found to differentiate between newborn-related AS and QS states with 87% and 80% agreement rates in comparison to PSG sleep state coding (Isler et al., 2016). With a growing industry of wearable technology and increasing need to monitor vital signs, the feasibility of RR measurement with triaxial ACCs has been confirmed (Bates et al., 2010; Lapi et al., 2014). Studies conducted in adults report acquiring good RR detection agreement rates

between ACCs (placed on the chest) and clinically validated RR measurement parameters, such as photoplethysmography (mean absolute error: 2.56 breaths/minute) (Jarchi et al., 2018) and a spirometer (mean absolute error: 0.53%) (Fekr et al., 2014). In latest studies, the fusion of ACC and GYRO axes has been reported to enhance RR detection precision with average error rates of 0.77 breaths/minute (Wang et al., 2018) and 0.70 breath/minute (Shen et al., 2017). We however, considered sensor fusion unnecessary, as the mean dominant delta RR calculated for the GYRO's Y (-1.8 breaths/minute) axis was significantly lower than all ACC channels. Furthermore, such as is in the case of the present study, Tadi et al., (2016) concluded that GYROs may achieve higher SNRs for being insusceptible to earth gravity and consuming more power as active sensors, unlike passive sensor ACCs.

4.2.2 Previous Validation of the MS for RR Detection in Older Subjects

A recent study comparing the MS to a clinically used respiratory inductance plethysmography (RIP) belt and Emfit pressure sensor, concluded that dominant delta RRs measured in older children were slightly lower within the ACC Y channel than in GYRO channels (Pakkala 2018). However, when compared to a nasal airflow pressure sensor, the MS's GYRO acquired the highest levels of agreement in terms of RR detection efficacy. Also, SNR values and PLVs were highest among ACC Y channel signals when compared with the Emfit and nasal pressure sensors. Conversely, ACC XY and GYRO XY channels had better SNR values than the RIP belt. In light of our findings, these apparent discrepancies are most likely explained by the location of the sensor in regard to abdominal breathing movements, as well as possible differences in respiration movements in young infants versus older children.

4.2.3 Infant Home Monitoring with Tools Available for Consumers

During the literature search, we also found a variety of wearable systems marketed to consumers with indications to monitor overall infant health. For example, the MonBaby (www.monbaby.com) utilizes a MEMS ACC, which is clipped on to a suit worn by the child to record breathing, movement and sleeping position data, which is then displayed on a tethered smartphone application (Aliverti, 2017). However, as is the case with most marketed wearable systems (Bonafide et al.,2017), the MonBaby lacks clinical benchmarking and validation, and has not been approved by any authorities to be used as a medical device. Interestingly, Bonafide et al., argue over the harmful effects that

constant home-monitoring of healthy infants have on both babies and parents. Moreover, the authors express their concerns on extreme parental anxiety caused by false baby monitor alarms, which in the worst-case scenario lead to needless and possibly harmful medical tests for the baby. However, with the expanding market of wearables and increasing parental wish to monitor infant health, a validated medical device (i.e. evaluated for effectiveness, accuracy and safety) for reliable in-home monitoring should be developed.

4.3 Justification of Contact Monitoring and Parental Perception

The actidiaper used in the study belongs to the category of contact monitoring methods, which means that it requires physical connection to the infant, in this case around the waistline. The main disadvantage of direct contact measurement techniques includes discomfort or poor toleration. However, in comparison to non-attached monitoring methods, direct contact techniques are less affected by the external environment and not as complex to interpret (Zhu et al., 2015). To assess parental attitudes and preconceptions of contact monitoring, user-experience questionnaires were handed out to the parents of the participants. According to the feedback received, the parents were highly compliant to the user instructions and indications given by the researchers. Despite initial hesitation regarding the tightness level of the actidiaper's waistband, no discomfort or change in the behavior of the infant was perceived while using the actidiaper. Conversely, parents were burdened by having to check the BLE connection status of the SleepSense application every once in a while. In addition, event logging was regarded as clumsy, especially during night feedings/awakenings. Therefore, to use the actidiaper for longer time periods, the parents would like for the BLE transmission range to be increased and to avoid having to log events.

4.4 Future Development

Accordingly, because the MS proved reliability in recording infant sleep-related RR and HR in both laboratory and home environments, future development aims should include improving the BLE connection stability of the MS or increasing the capacity of the MS's internal memory to reduce BLE connection dependence. More efforts should be put into optimizing the skin-sensor interphase, including testing of different adhesive materials for better long-term ECG signal stability. Moreover, textile electrodes are generally considered less irritating to infant skin (Zhu et al., 2015), which supports their further development to optimize signal quality and other properties as a wearable

device. Finally, the SleepSense application needs a more consumer-friendly design.

4.5 Concluding Remarks

Overall, the MS has the potential to provide a handy and objective tool for studying sleep structure and development in infants over long time periods, and possibly liberating fatigued parents from filling in sleep diaries and follow-up questionnaires. Moreover, the reported 25% of predominantly Caucasian and 50% of predominantly Asian parents (Mindell et al., 2010) claiming to have infants whom sleep poorly may receive answers to verify their concerns. In the future, data obtained from the ongoing in-hospital PSG/MS recordings, during which sleep states are clinically classified based on a variety of physiological parameters, will be employed along with home recorded data to teach the MS to discard irrelevant and artifactual data and to detect different stages of sleep and activity automatically. Thus, home sleep monitoring, with a version of the actidiaper that automatically detects different sleep states, could bring added value and further reliability to clinical sleep studies. Moreover, the actidiaper also has the potential to be used as a companion diagnostic tool for infant cardiorespiratory and movement disorders. Robust clinical testing and larger study populations are, however, needed to further validate the actidiaper for clinical diagnostic purposes.

5. Acknowledgements

I would first like to thank my supervisor, Sampsa Vanhatalo, for giving me the opportunity to be part of such a diverse and talented team. His encouragement and guidance in this project have been irreplaceable. Next, I would like to thank my other supervisor, Jukka Ranta, who was always there to ease my struggles with MATLAB and offer both emotional and peer support. A special thank you also goes to all my co-workers at BABA Center for the inspiring teamwork and enjoyable working atmosphere. Last but not least, I would like to give a round of applause to all the volunteering families for making this study possible.

6. References

Aliverti A (2017) Wearable technology: role in respiratory health and disease. *Breathe (Sheff)* 13: e27-e36

Anders TF, Emde R, Parmelee A. Los Angeles: UCLA Brain Information Service (1971) A manual of standardized terminology, techniques and criteria for scoring states of sleep and wakefulness in newborn infants.

Anders TF (1978) Home-recorded sleep in 2- and 9-month-old infants. J Am Acad Child Psychiatry 17: 421-432

Anders TF & Keener M (1985) Developmental course of night-time sleep-wake patterns in full-term and premature infants during the first year of life. I. Sleep. 8: 173–192

Assefa SZ, Diaz-Abad M, Wickwire EM, & Scharf SM (2015) The Functions of Sleep. AIMS Neuroscience. 2: 155-171

Barbeau DY & Weiss MD (2017) Sleep Disturbances in Newborns. Children (Basel) 4: 10.3390/children4100090

BATES A, Ling MJ, Mann J, Arvind DK (2010) Respiratory rate and flow waveform estimation from tri-axial accelerometer data**.** Body Sensor Networks (BSN), International Conference, pp. 144-150

Bathory E & Tomopoulos S (2017) Sleep Regulation, Physiology and Development, Sleep Duration and Patterns, and Sleep Hygiene in Infants, Toddlers, and Preschool-Age Children. Curr Probl Pediatr Adolesc Health Care 47: 29-42

Bernier A, Carlson SM, Bordeleau S, & Carrier J (2010) Relations between physiological and cognitive regulatory systems: infant sleep regulation and subsequent executive functioning. Child Dev 81: 1739-1752

Bonafide, C. P., Jamison, D. T., & Foglia, E. E. (2017). The Emerging Market of Smartphone-Integrated Infant Physiologic Monitors. *JAMA*, *317*(4), 353-354

Bouwstra S, Chen W, Feijs L, & Oetomo SB (2009) Smart jacket design for neonatal monitoring with wearable sensors. IEEE Body Sens. Netw. 40: 162–167

Buxton OM, Cain SW, O'Connor SP, Porter JH, Duffy JF, Wang W, Czeisler CA, & Shea SA (2012) Adverse metabolic consequences in humans of prolonged sleep restriction combined with circadian disruption. Science translational medicine 4: 1-10

Cao H, Hsu LC, Ativanichayaphong T, Sin J, & Chiao JC (2007) A non-invasive and remote infant monitoring system using CO2 sensors. In Proceedings of the IEEE SENSORS 2007 Conference, Atlanta, GA, USA, 28–31 October 2007: pp. 989–992

Chan M, Esteve D, Fourniols JY, Escriba C, & Campo E (2012) Smart wearable systems: current status and future challenges. Artif Intell Med 56: 137-156

Chen H, Xue M, Mei Z, Bambang Oetomo S, & Chen W (2016) A Review of Wearable Sensor Systems for Monitoring Body Movements of Neonates. Sensors (Basel) 16: 10.3390/s16122134

Chouchou F & Desseilles M (2014) Heart rate variability: a tool to explore the sleeping brain? Front Neurosci 8: 402

Cirelli C & Tononi G (2008) Is sleep essential? PLOS Biology 6: 1–7

Dahl RE (1996) The impact of inadequate sleep on children's daytime cognitive function. Semin Pediatr Neurol 3: 44-50

Dattilo M, Antunes HK, Medeiros A, Monico-Neto M, Souza Hde S, Lee KS, Tufik S, & de Mello MT (2012) Paradoxical sleep deprivation induces muscle atrophy. Muscle Nerve 45: 431-433

Davis KF, Parker KP, & Montgomery GL (2004) Sleep in infants and young children: Part one: normal sleep. J Pediatr Health Care 18: 65-71

de Beer NA, Andriessen P, Berendsen RC, Oei SG, Wijn PF, & Oetomo SB (2004) Customized spectral band analysis compared with conventional Fourier analysis of heart rate variability in neonates. Physiol Meas 25: 1385-1395

Douglas PS & Hill PS (2013) Behavioral sleep interventions in the first six months of life do not improve outcomes for mothers or infants: a systematic review. Journal of Developmental & Behavioral Pediatrics. 34: 497–507

Faraut B, Boudjeltia KZ, Vanhamme L, & Kerkhofs M (2012) Immune, inflammatory and cardiovascular consequences of sleep restriction and recovery. Sleep Med Rev 16: 137-149

Fekr AR, Janidarmian M, Radecka K, & Zilic Z (2014) A medical cloud-based platform for respiration rate measurement and hierarchical classification of breath disorders. *Sensors, 14*: 11204-11224

Ficca G, Fagioli I, & Salzarulo P (2000) Sleep organization in the first year of life: developmental trends in the quiet sleep-paradoxical sleep cycle. J Sleep Res 9: 1-4

Field T (2017) Infant sleep problems and interventions: A review. Infant Behavior and Development. 40: 40-53

Galland BC, Kennedy GJ, Mitchell EA, & Taylor BJ (2012a) Algorithms for using an activity-based accelerometer for identification of infant sleep-wake states during nap studies. Sleep Med 13: 743-751

Galland BC, Taylor BJ, Elder DE, Herbison P (2012b) Normal sleep patterns in infants and children: a systematic review of observational studies. Sleep Med Rev. 16: 213–22

Goodlin-Jones BL, Burnham MM, Gaylor EE, & Anders TF (2001) Night waking, sleep-wake organization, and self-soothing in the first year of life. J Dev Behav Pediatr 22: 226-233

Grigg-Damberger MM (2016) The Visual Scoring of Sleep in Infants 0 to 2 Months of Age. J Clin Sleep Med 12: 429-445

Harper RM, Schechtman VL, & Kluge KA (1987) Machine classification of infant sleep state using cardiorespiratory measures. Electroencephalogr Clin Neurophysiol 67: 379-387

Heimann K, Heussen N, Vaessen P, Wallmeier C, Orlikowsky T, & Wenzl TG (2013) Basic values for heart and respiratory rates during different sleep stages in healthy infants. Biomed Tech (Berl) 58: 27-34

Hurtado JM, Rubchinsky LL, & Sigvardt KA (2004) Statistical method for detection of phase-locking episodes in neural oscillations. J Neurophysiol 91: 1883-1898

Isler JR, Thai T, Myers MM, & Fifer WP (2016) An automated method for coding sleep states in human infants based on respiratory rate variability. Dev Psychobiol 58: 1108-1115

Korotchikova I, Stevenson NJ, Livingstone V, Ryan CA, & Boylan GB (2016) Sleep-wake cycle of the healthy term newborn infant in the immediate postnatal period. Clin Neurophysiol 127: 2095-2101

Lachaux JP, Rodriguez E, Martinerie J, Varela FJ (1999) Measuring phase synchrony in brain signals. Hum. Brain Mapp. 8:194–208

Lachaux JP, Rodriguez E, Van Quyen ML, Lutz A, Martinerie J, Varela FJ (2000) Studying single-trials of phase synchronous activity in the brain. International Journal of Bifurcation and Chaos 10: 2429-2439

Lapi S, Lavorini F, Borgioli G, Calzolai M, Masotti L, Pistolesi M & Fontana GA (2014) Respiratory rate assessments using dual-accelerometer device. Respiratory Physiology & Neurobiology 191: 60-66

Linti C, Horter H, Österreicher P, & Planck H (2006) Sensory baby vest for the monitoring of infants. In Proceedings of the International Workshop on Wearable and Implantable Body Sensor Networks (BSN'06), Cambridge, MA, USA, 3–5 April 2006: pp. 3–137

Meltzer LJ, Montgomery-Downs HE, Insana SP, & Walsh CM (2012) Use of actigraphy for assessment in pediatric sleep research. Sleep Med Rev 16: 463-475

Mindell JA, Owens JA, Carskadon MA (1999) Developmental features of sleep. Child Adolesc Psychiatr Clin 8: 695–725

Mindell JA, Sadeh A,Wiegand B (2010) Cross-cultural differences in infant and toddler sleep. *Sleep Med* 11:274-80

Mindell JA & Lee C (2015) Sleep, mood, and development in infants. Infant Behav Dev 41: 102-107

Mirmiran M, Baldwin RB, & Ariagno RL (2003) Circadian and sleep development in preterm infants occurs independently from the influences of environmental lighting. Pediatr Res 53: 933-938

Mormann F, Lehnertz K, David P, Elger EC (2000) Mean phase coherence as a measure for phase synchronization and its application to the eeg of epilepsy patients. Physica D: Nonlinear Phenomena 144:358–369

Mouthon AL & Huber R (2015) Methods in pediatric sleep research and sleep medicine. Neuropediatrics 46: 159-170

Movesense Sensor Datasheet. Movesense: (https://www.movesense.com/wp-content/uploads/2017/11/Movesense-Sensor-Datasheet-_-20171109.pdf) read: 22.01.2019

Myers MM, Fifer WP, Grose-Fifer J, Sahni R, Stark RI, & Schulze KF (1997) A novel quantitative measure of Trace-alternant EEG activity and its association with sleep states of preterm infants. Dev Psychobiol 31: 167-174

Mäkelä TE, Peltola MJ, Nieminen P, Paavonen EJ, Saarenpää-Heikkilä O, Paunio T, & Kylliäinen A (2018) Night awakening in infancy: Developmental stability and longitudinal associations with psychomotor development. Dev Psychol 54: 1208-1218

Pakkala O (2018) The Suitability of the Movesense Sensor for Breathing Examination. Engineering Thesis of Health Technology, Metropolia University of Applied Sciences.

Palmstierna P, Sepa A, & Ludvigsson J (2008) Parent perceptions of child sleep: a study of 10,000 Swedish children. Acta Paediatr 97: 1631-1639

Patel S, Park H, Bonato P, Chan L, Rodgers M (2012) A review of wearable sensors and systems with application in rehabilitation. J. Neuroeng. Rehabil. 9: 21–38

Prechtl HF (1974) The behavioural states of the newborn infant (a review). Brain Res 76: 185-212

Ranta J (2018) Sleep Classification in Infants Using a Bed Mattress Sensor and Analysis of ECG. Master's Thesis: Degree Programme in Life Science Technologies. School of Science, Aalto University

Rimet Y, Brusquet Y, Ronayette D, Dageville C, Lubrano M, Mallet E, Rambaud C, Terlaud C, Silve J, Lerda O et al (2007) Surveillance of infants at risk of apparent life-threatening events (ALTE) with the BBA bootee: A wearable multiparameter monitor. In Proceedings of the 29th Annual International Conference of the IEEE EMBS, Cité Internationale, Lyon, France, 23–26 August 2007: pp. 4997–5000

Sazonova NA, Sazonov ES, Schuckers SAC (2002) Activity-Based Sleep-Wake Identification in Infants. Computers in Cardiology 29: 525-528

Sadeh A, Acebo C, Seifer R, Aytur S, & Carskadon MA (1995) Activity-based assessment of sleep-wake patterns during the 1st year of life. Infant Behavior and Development. 18: 329–337

Sadeh A (2015) Iii. Sleep assessment methods. Monogr Soc Res Child Dev 80: 33-48

Shaffer F & Ginsberg JP (2017) An Overview of Heart Rate Variability Metrics and Norms. Front Public Health 5: 258

Scher A (2005) Infant sleep at 10 months of age as a window to cognitive development. Early Hum Dev 81: 289-292

Schulz KF, Grimes DA (2005): Multiplicity in randomized trials I: endpoints and treatments. Lancet 365:1591-1595

Skeldon AC, Derks G, & Dijk DJ (2016) Modelling changes in sleep timing and duration across the lifespan: Changes in circadian rhythmicity or sleep homeostasis? Sleep Med Rev 28: 96-107

So K, Buckley P, Adamson TM, & Horne RS (2005) Actigraphy correctly predicts sleep behavior in infants who are younger than six months, when compared with polysomnography. Pediatr Res 58: 761-765

Southall DP, Richards JM, Shinebourne EA, Franks CI, Wilson AJ, & Alexander JR (1983) Prospective population-based studies into heart rate and breathing patterns in newborn infants: Prediction of infants at risk of SIDS. Tildon JY, Roeder LM, Steinschneider A; editors. Sudden infant death syndrome. Academic Press; New York, NY: pp. 621-651

Spruyt K, Aitken RJ, So K, Charlton M, Adamson TM, & Horne RS (2008) Relationship between sleep/wake patterns, temperament and overall development in term infants over the first year of life. Early Hum Dev 84: 289-296

Streiner DL & Norman GR (2011) Correction for Multiple Testing: Is There a Resolution? Chest 140: 16-18

Tadi MJ, Lehtonen E, Teuho J, Saraste A, Pänkäälä M, Teräs M & Koivisto T (2016) A Miniaturized MEMS Motion Processing System for Nuclear Medicine Imaging Applications. In Proceedings of the Computing in Cardiology Conference (CinC), 11-14 Sept. 2016, Vancouver, BC, Canada

Tass P, Rosenblum MG, Weule J, Kurths J, Pikovsky A, Volkmann J, Schnitzler A, Freund HJ (1998) Detection of n:m Phase Locking from Noisy Data: Application to Magnetoencephalography. Physical Review Letters 81: 3291—3294

Terrill PI, Wilson SJ, Suresh S, Cooper DM, & Dakin C (2012) Application of recurrence quantification analysis to automatically estimate infant sleep states using a single channel of respiratory data. Med Biol Eng Comput 50: 851-865

Tham EK, Schneider N, & Broekman BF (2017) Infant sleep and its relation with cognition and growth: a narrative review. Nat Sci Sleep 9: 135-149

Tokariev A, Palmu K, Lano A, Metsaranta M, & Vanhatalo S (2012) Phase synchrony in the early preterm EEG: development of methods for estimating synchrony in both oscillations and events. Neuroimage 60: 1562-1573

van den Hoogen A, Teunis CJ, Shellhaas RA, Pillen S, Benders M, & Dudink J (2017) How to improve sleep in a neonatal intensive care unit: A systematic review. Early Hum Dev 113: 78-86

Wang S, Liu M, Pang B, Li P, Yao Z, Zhang X, Chen H (2018) A new physiological signal acquisition patch designed with advanced respiration monitoring algorithm based on 3-axis accelerator and gyroscope. In Proceedings of the 40th Annual International Conference of the IEEE Engineering in Medicine and Biology Society (EMBC), Honolulu, HI, USA, 18–21 July 2018: pp. 441–444

Weinraub M, Bender RH, Friedman SL, Susman EJ, Knoke B, Bradley R, Houts R, & Williams J (2012) Patterns of developmental change in infants' nighttime sleep awakenings from 6 through 36 months of age. Dev Psychol 48: 1511-1528

Werth J, Long X, Zwartkruis-Pelgrim E, Niemarkt H, Chen W, Aarts RM, & Andriessen P (2017) Unobtrusive assessment of neonatal sleep state based on heart rate variability retrieved from electrocardiography used for regular patient monitoring. Early Hum Dev 113: 104-113

Yasuma F & Hayano J (2004) Respiratory sinus arrhythmia: why does the heartbeat synchronize with respiratory rhythm? Chest 125: 683-690

Zhu Z, Liu T, Li G, Li T, & Inoue Y (2015) Wearable sensor systems for infants. Sensors (Basel) 15: 3721-3749

7. Supplementary Material

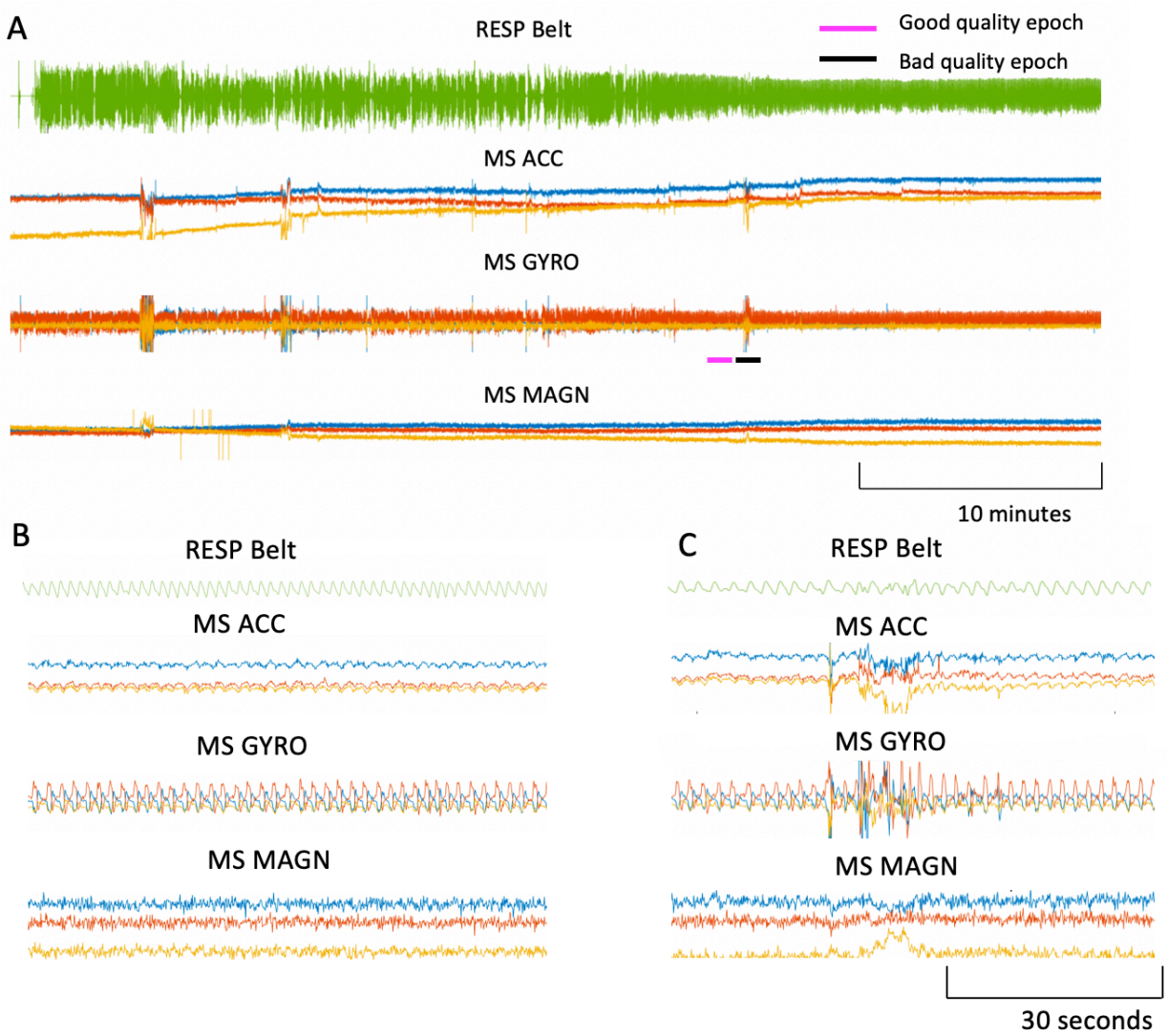

Figure 10. An example of the selection criteria of time synchronized signal epochs to be filtered and analyzed in part 1 of the study. Graph A includes the RESP belt signal and all MS channel signals. The pink bar beneath the MS GYRO signals outlines an epoch of good quality (respiration) signal that has been selected for further analysis, whereas the black bar outlines an epoch that has been discarded from further analysis due to a movement artifact. Magnifications of the corresponding signals are shows in graphs B (included epoch) and C (excluded epoch). The horizontal axes of all graphs (A-C) depict time (A = minutes; B and C = seconds). In A-C: RESP belt signal = green, and, yellow = Z-axis, blue = X-axis and red = Y-axis of all MS channels.

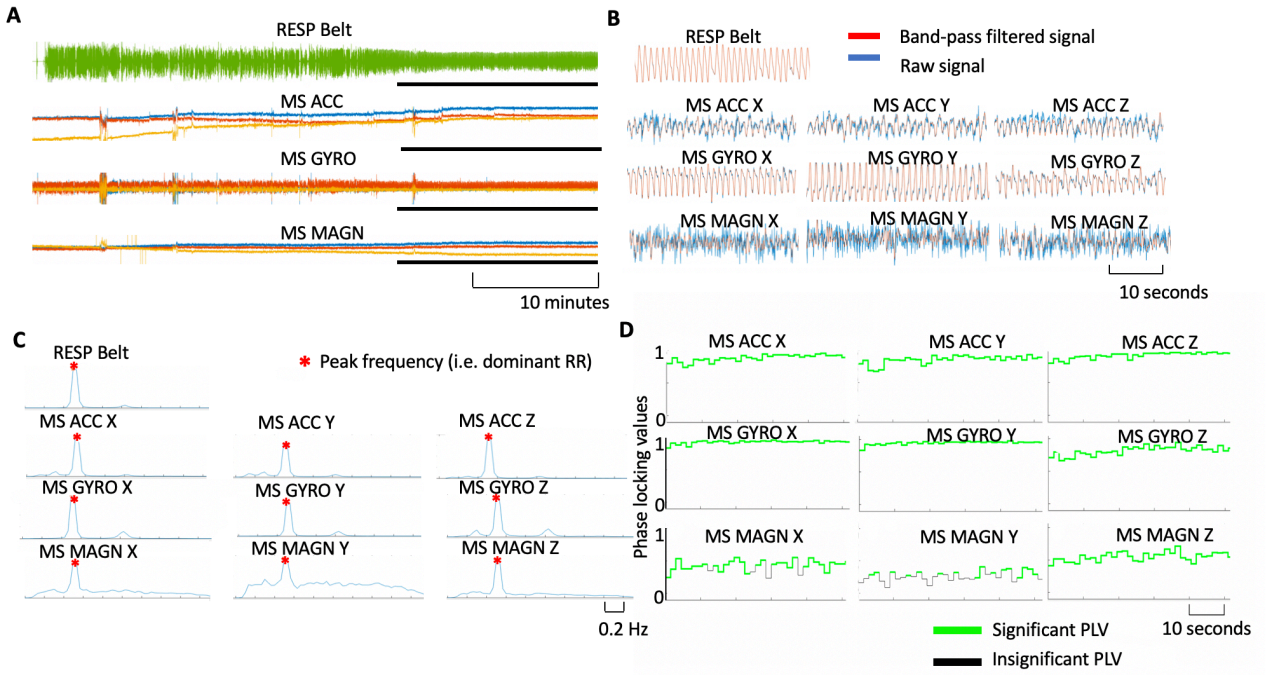

Figure 11. An example of part 1 respiratory signal analysis outputs (N=1). Graph A includes time synchronized outputs of the RESP belt (green) and all MS (X = blue; Y = red; Z = yellow) channels. The black bars beneath each signal highlight the location of a manually selected epoch of good quality respiration signal to be filtered and analyzed. Graph B contains a magnification of the corresponding band-pass filtered (high-pass cut-off point = 0.1 Hz; low-pass cut-off point= 2 Hz) signals (red) and raw signals (blue) within the chosen epoch. Graph C contains illustrations of the power spectrums of a 30-second segment within the chosen epoch. The red asterisks indicate peak frequencies, which were taken as the representative of dominant RR, and used to calculate the SNR of each 30-second segment. Graph D contains a representation of the PLVs calculated for the MS signals of the chosen epoch, which was divided into 30-second-long segments and the PLVs were calculated for each segment. The green portions of the signals denote epochs with statistically significant PLVs, whereas the black portions of the signals denote epochs with statistically insignificant PLVs. The horizontal axes in graphs A, B and D represent time (A = minutes; B and D = seconds), and frequency (Hz) in graph C. In graph D, the horizontal Y axes represent PLVs, ranging from 0 (no phase locking) to 1 (complete phase locking).

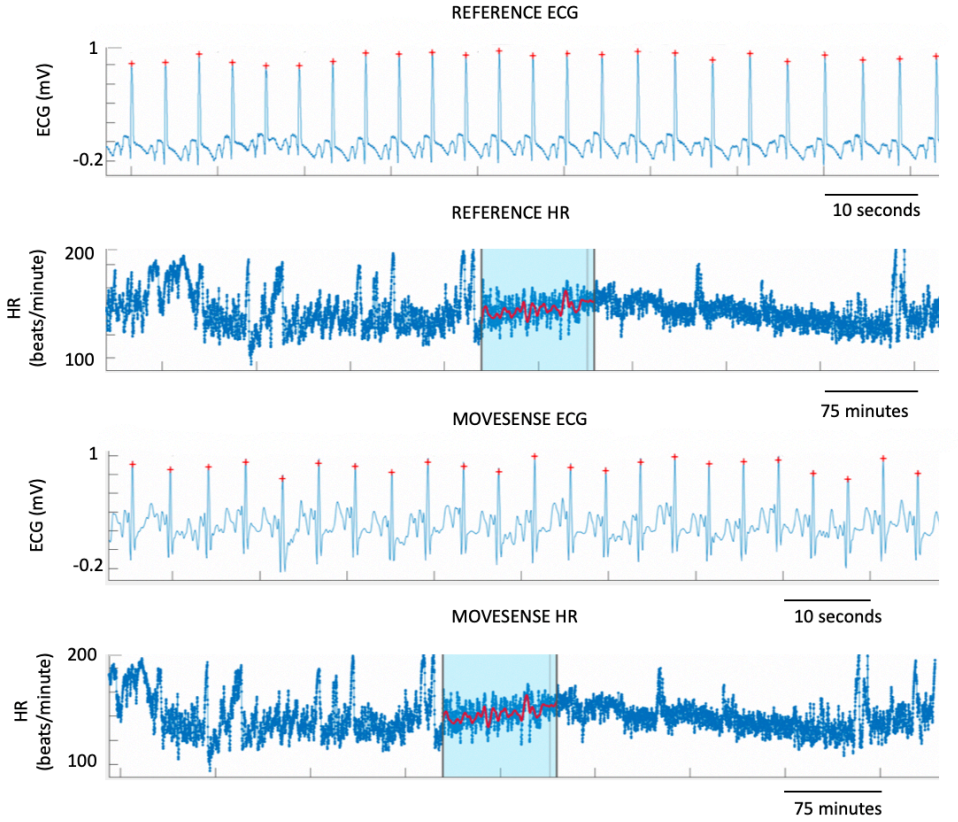

Figure 12. An example of the reference and MS ECG and HR signal outputs used for the HRV analysis (N=1). The light blue boxes and red traces seen in the HR graphs highlight the selected 10-minute HRV analysis windows. The thin vertical grey lines within the analysis window represent the ranges of the ECG graphs. The red crosses on the ECG graphs denote detected R-peaks. Horizontal axes represent time (ECG graphs = seconds; HR graphs = minutes), and vertical axes represent voltage (ECG) and beats/minute (HR).

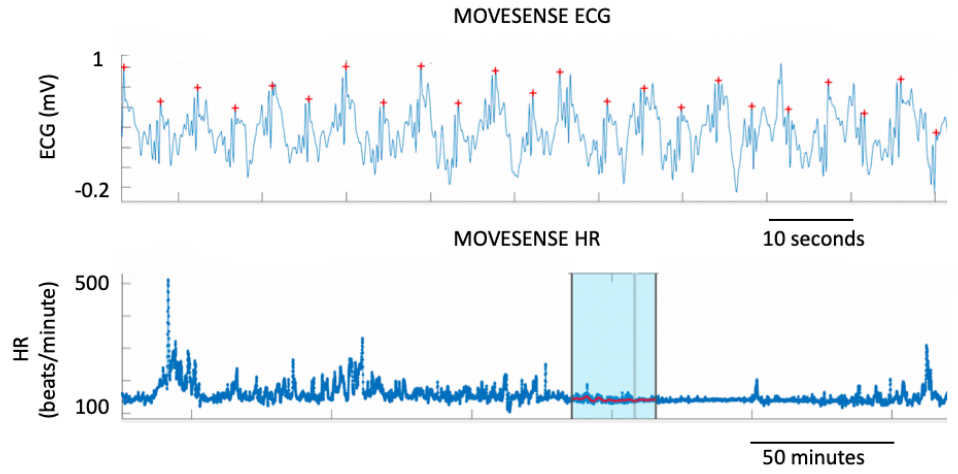

Figure 13. An example of the ECG and HR outputs of a study subject excluded from the HRV analysis. The ECG signal is artifactual due to unattached contact between the skin and textile electrodes of the actidiaper. See Figure 12 for more details.